HyperSINDy: Deep Generative Modeling of Nonlinear Stochastic Governing Equations

Mozes Jacobs
Harvard University
mozesjacobs@g.harvard.edu

Bingni W. Brunton
University of Washington
bbrunton@uw.edu

Steven L. Brunton
University of Washington
sbrunton@uw.edu

J. Nathan Kutz
University of Washington
kutz@uw.edu

Ryan V. Raut
Allen Institute
ryan.raut@alleninstitute.org

Abstract

The discovery of governing differential equations from data is an open frontier in machine learning. The *sparse identification of nonlinear dynamics* (SINDy) [Brunton et al., 2016] framework enables data-driven discovery of interpretable models in the form of sparse, deterministic governing laws. Recent works have sought to adapt this approach to the stochastic setting, though these adaptations are severely hampered by the curse of dimensionality. On the other hand, Bayesian-inspired deep learning methods have achieved widespread success in high-dimensional probabilistic modeling via computationally efficient approximate inference techniques, suggesting the use of these techniques for efficient stochastic equation discovery. Here, we introduce *HyperSINDy*, a framework for modeling stochastic dynamics via a deep generative model of sparse governing equations whose parametric form is discovered from data. HyperSINDy employs a variational encoder to approximate the distribution of observed states and derivatives. A hypernetwork [Ha et al., 2016] transforms samples from this distribution into the coefficients of a differential equation whose sparse form is learned simultaneously using a trainable binary mask [Louizos et al., 2018]. Once trained, HyperSINDy generates stochastic dynamics via a differential equation whose coefficients are driven by a Gaussian white noise. In experiments, HyperSINDy accurately recovers ground truth stochastic governing equations, with learned stochasticity scaling to match that of the data. Finally, HyperSINDy provides uncertainty quantification that scales to high-dimensional systems. Taken together, HyperSINDy offers a promising framework for model discovery and uncertainty quantification in real-world systems, integrating sparse equation discovery methods with advances in statistical machine learning and deep generative modeling.

1 Introduction

Across numerous disciplines, large amounts of measurement data have been collected from dynamical phenomena lacking comprehensive mathematical descriptions. It is desirable to model these data in terms of governing equations involving the state variables, which typically enables insight into the physical interactions in the system. To this end, recent years have seen considerable progress in the ability to distill such governing equations from data alone (e.g., [Schmidt and Lipson, 2009, Brunton et al., 2016]). Nonetheless, this remains an outstanding challenge for systems exhibiting apparently stochastic nonlinear behavior, particularly when lacking even partial knowledge of the governing equations. Such systems thus motivate probabilistic approaches that not only reproduce the observed stochastic behavior (e.g., via generic stochastic differential equations (SDEs) [Friedrich et al., 2011] or neural networks [Girin et al., 2021, Lim and Zohren, 2021]), but do so via discovered analytical representations that are parsimonious and physically informative [Boninsegna et al., 2018].

We are particularly interested in model-free methods that seek to discover both the parameters and functional form of governing equations describing the data. To this end, the sparse identification of nonlinear dynamics (SINDy) framework [Brunton et al., 2016] has emerged as a powerful data-driven approach that identifies both the coefficients and terms of differential equations, given a pre-defined library of candidate functions. The effectiveness of SINDy for sparse model discovery derives from the tendency of physical systems to possess a relatively limited set of active terms. Extensions of the SINDy framework have sought to increase its robustness to noise, offer uncertainty quantification (UQ), and make it suitable for modeling stochastic dynamics [Boninsegna et al., 2018, Niven et al., 2020, Messenger and Bortz, 2021, Hirsh et al., 2021, Callaham et al., 2021, Fasel et al., 2022, Wang et al., 2022]. However, these extensions have generally relied upon computationally expensive approaches to learn the appropriate probability distributions. As such, a unified and computationally tractable formulation of SINDy that meets these additional goals is presently lacking.

Variational inference (VI) methods represent a class of techniques for addressing the complex and often intractable integrals arising in exact Bayesian inference, instead approximating the true posterior via simple distribution(s). Recently, the combination of *amortized* VI [Ganguly et al., 2022] with the representational capacity of neural networks has emerged as a powerful, efficient approach to probabilistic modeling, with widespread application in the form of deep generative models [Kingma and Welling, 2014, Rezende and Mohamed, 2015]. Despite the success of these approaches for dynamical modeling (e.g., [Girin et al., 2021]), applications thus far have utilized generic state space formulations or parameter inference on a known functional form of the dynamics. Thus, the potential for VI to facilitate probabilistic equation discovery remains largely unexplored.

1.1 Contributions

In this work, we propose HyperSINDy, a VI-based SINDy implementation that learns a parameterized distribution of ordinary differential equations (ODEs) sharing a common sparse form. Specifically, HyperSINDy employs a variational encoder to parameterize a latent distribution over observed states and derivatives, then uses a hypernetwork [Ha et al., 2016, Pawlowski et al., 2018] to translate samples from this distribution into the coefficients of a sparse ODE whose functional form is learned in a common optimization. In this way, HyperSINDy is able to model complex stochastic dynamics through an interpretable analytical expression – technically, a *random* ODE [Han and Kloeden, 2017] – whose coefficients are parameterized by a white noise process.

Specific contributions of the HyperSINDy framework include:

- **Efficient and Accurate Modeling of Stochastic Dynamics at Scale.** Through VI, we circumvent the curse of dimensionality that hampers other methods in identifying sparse stochastic equations. Specifically, HyperSINDy can accurately discover governing equations for stochastic systems having well beyond two spatial dimensions, which existing approaches have not exceeded [Boninsegna et al., 2018, Callaham et al., 2021, Wang et al., 2022, Huang et al., 2022, Tripura and Chakraborty, 2023]. Importantly, HyperSINDy's generative model is able to learn a complex distribution over the coefficients, and variance proportionately scales to match that of the data.
- **Generative Modeling of Dynamics.** Once trained, HyperSINDy generates a random dynamical system whose vector field is parameterized by a Gaussian white noise. Hence, our approach efficiently arrives at a generative model for both the system dynamics and the exogenous disturbances (representing, e.g., unresolved scales). This permits simulations that reproduce the stochastic dynamical behavior of the observed process, while providing a natural method for quantifying uncertainty of the model parameters and propagating uncertainty in the probabilistic model forecast.
- **Interpretable Governing Equations Discovery.** In contrast to other deep generative approaches for modeling stochastic dynamics, HyperSINDy discovers the analytical form of a sparse governing equation without a priori knowledge. Sparsity promotes human readable models where each term corresponds to an interpretable physical mechanism. This notion of interpretability, based on sparsity, is appealing in the traditional perspective of engineering and physics.

In section 1.2, we discuss relevant literature. In section 2, we provide a background on the specific methods and mathematics that inspired our method. In section 3, we describe HyperSINDy. In section 4, we show results on various experiments. In section 5, we conclude with a discussion of our method, its limitations, and possible future directions.

1.2 Related Work

HyperSINDy bridges two parallel lines of work concerning data-driven modeling for stochastic dynamics: namely, probabilistic sparse equation discovery and deep generative modeling.

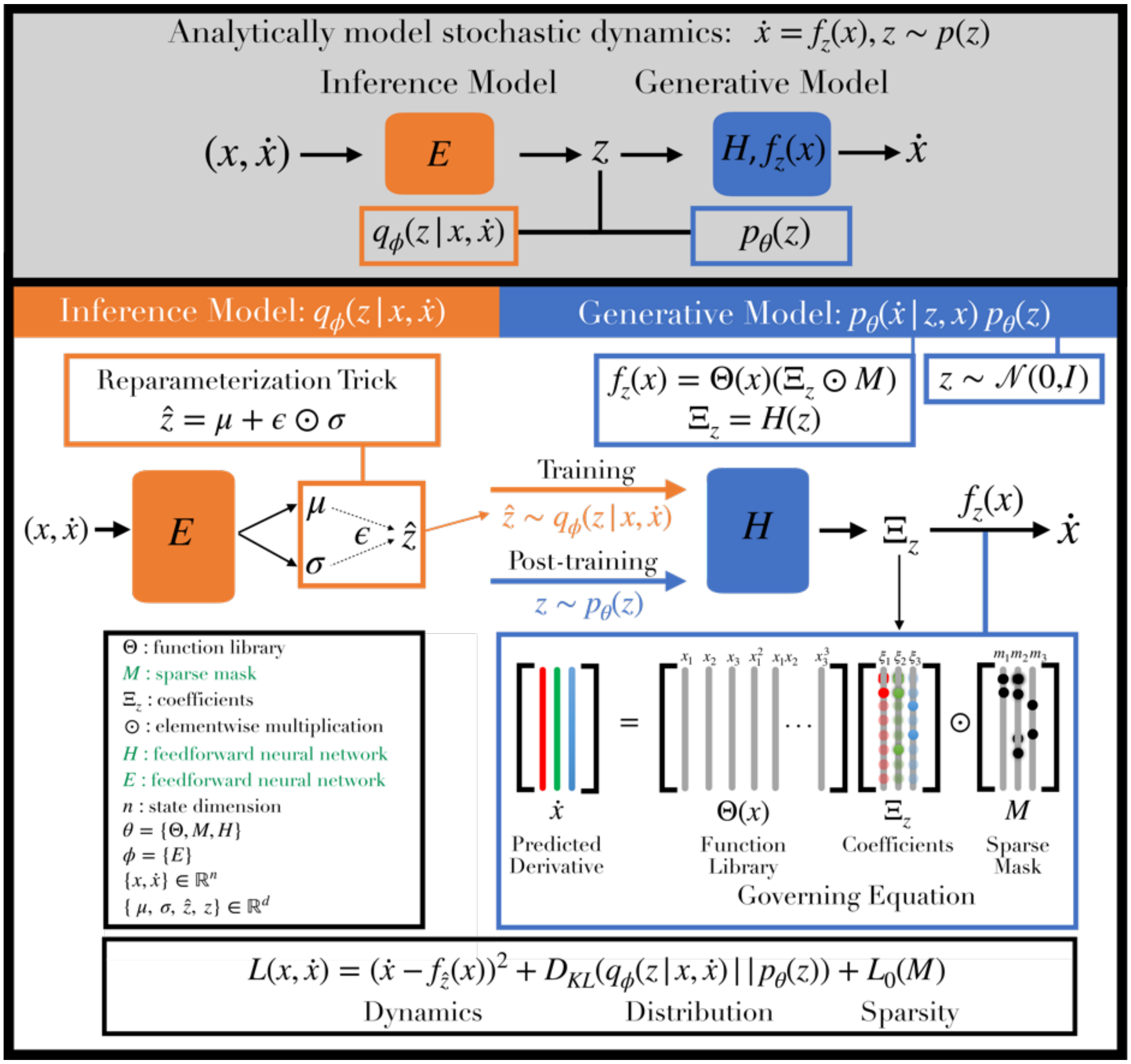
Analytically model stochastic dynamics: $\dot{x} = f_z(x), z \sim p(z)$
Inference Model
Generative Model
$(x, \dot{x})$
E
z
$H, f_z(x)$
$\dot{x}$
$q_\phi(z \mid x, \dot{x})$
$p_\theta(z)$
Inference Model: $q_\phi(z \mid x, \dot{x})$
Generative Model: $p_\theta(\dot{x} \mid z, x)\, p_\theta(z)$
Reparameterization Trick
$\hat{z} = \mu + \epsilon \odot \sigma$
$f_z(x) = \Theta(x)(\Xi_z \odot M)$
$\Xi_z = H(z)$
$z \sim \mathcal{N}(0, I)$
μ
σ
ϵ
$\hat{z}$
Training
$\hat{z} \sim q_\phi(z \mid x, \dot{x})$
Post-training
$z \sim p_\theta(z)$
H
Ξ_z
$f_z(x)$
Θ : function library
M : sparse mask
Ξ_z : coefficients
$\odot$: elementwise multiplication
H : feedforward neural network
E : feedforward neural network
n : state dimension
$\theta = \{\Theta, M, H\}$
$\phi = \{E\}$
$\{x, \dot{x}\} \in \mathbb{R}^n$
$\{\mu, \sigma, \hat{z}, z\} \in \mathbb{R}^d$
x_1 x_2 x_3 x_1^2 x_1x_2 x_3^3
$\xi_1 \xi_2 \xi_3$
$m_1 m_2 m_3$
$\dot{x}$
Predicted Derivative
$\Theta(x)$
Function Library
Ξ_z
Coefficients
M
Sparse Mask
Governing Equation
$L(x, \dot{x}) = (\dot{x} - f_{\hat{z}}(x))^2 + D_{KL}(q_\phi(z \mid x, \dot{x}) \,||\, p_\theta(z)) + L_0(M)$
Dynamics
Distribution
Sparsity

Figure 1: **HyperSINDy Framework**. HyperSINDy employs an inference model and generative model to discover an analytical representation of observed stochastic dynamics in the form of a random (nonlinear) ODE $f_{\mathbf{z}}(x)$. The inference model is an encoder neural network that maps $(\mathbf{x}, \dot{\mathbf{x}})$ to the parameters μ and σ of $q_\phi(\mathbf{z}|\mathbf{x}, \dot{\mathbf{x}})$. $\hat{\mathbf{z}}$ can be sampled using a simple reparameterization of μ and σ. The generative model predicts the derivative via a hypernetwork H, which transforms $\mathbf{z}$ into $\Xi_{\mathbf{z}}$, the coefficients of the ODE. $f_{\mathbf{z}}(\mathbf{x})$ comprises a function library Θ, the coefficients $\Xi_{\mathbf{z}}$, and sparse mask M. If $\dot{\mathbf{x}}$ is not available (e.g., after training), $\mathbf{z}$ is sampled from the prior $\mathbf{z} \sim p_\theta(\mathbf{z})$ to produce $\Xi_{\mathbf{z}}$. In the legend, trainable parameters are shown in green. The loss function comprises terms related to 1) the derivative reconstructions, 2) the latent distribution $q_\phi(\mathbf{z}|\mathbf{x}, \dot{\mathbf{x}})$, and 3) sparsity of the discovered equation. See accompanying pseudocode 1 and 2 for details on batch-wise training.

Most probabilistic implementations of SINDy have concerned UQ and noise robustness in the deterministic setting, rather than modeling stochastic dynamics per se. Of these approaches, ensembling methods [Fasel et al., 2022] have achieved state-of-the-art UQ and noise robustness for deterministic SINDy models, and were recently shown [Gao et al., 2023] to offer a computationally efficient alternative to earlier Bayesian implementations of SINDy [Niven et al., 2020, Hirsh et al., 2021] leveraging costly sampling routines to compute posterior distributions. Nonetheless, a model of the process noise is crucial for accurate UQ in the stochastic dynamics setting. Multiple studies have generalized the SINDy framework for the identification of parametric SDEs [Boninsegna et al., 2018, Callaham et al., 2021], with three such studies recently performed in the Bayesian setting [Wang et al., 2022, Huang et al., 2022, Tripura and Chakraborty, 2023]. However, as discussed in these works, existing methods for approximating the drift and diffusion terms of the SDE (e.g., constructing histograms for the Kramers-Moyal expansion) are severely hampered by the curse of dimensionality, with computational cost generally scaling exponentially with SDE state dimension. Thus, an efficient and scalable formulation of SINDy for stochastic dynamics remains lacking.

A separate line of work has leveraged advances in probabilistic deep learning for modeling stochastic dynamics, with deep generative models achieving state-of-the-art performance across a wide range of modeling tasks (e.g., [Yoon et al., 2019, Girin et al., 2021]). Although these models do not typically involve explicit dynamical representations, the new paradigm of physics-informed machine learning [Karniadakis et al., 2021] has motivated numerous developments at this intersection (e.g., [Lopez and Atzberger, 2021, Takeishi and Kalousis, 2021, Yang et al., 2020, Zhang et al., 2019]. Regarding the specific goal of (stochastic) equation discovery, several recent works have successfully employed VAEs to learn the coefficients of a generic (or pre-specified) SDE representation within a (potentially lower-dimensional) latent space[Hasan et al., 2022, García et al., 2022, Nguyen et al., 2021, Zhong and Meidani, 2023]. We propose to similarly leverage a VAE-like architecture to perform inference on a latent stochastic process; however, we seek to additionally discover a structural representation of the governing laws, which can yield considerable physical insight into the system [Boninsegna et al., 2018, Nayek et al., 2021, Wang et al., 2022]. Taken together, we seek to bridge the above fields via a unified deep learning architecture (trainable end-to-end with backpropagation) that enables discovery of the functional form of a governing stochastic process, along with posterior distributions over the discovered system coefficients (e.g., for UQ).

2 Background

We briefly overview the SINDy and VAE frameworks, as well as an implementation of an L_0 loss, before describing their integration within the HyperSINDy architecture.

Sparse Identification of Nonlinear Dynamics The SINDy [Brunton et al., 2016] framework leverages sparse regression to enable discovery of a parsimonious system of differential equations from time-ordered snapshots. Thus, consider a system with state $\mathbf{x}(t) \in \mathbb{R}^d$ governed by the ODE:

$$\dot{\mathbf{x}}(t) = f(\mathbf{x}(t)) \tag{1}$$

Given m observations of the system in time $\mathbf{X} = [\mathbf{x}(t_1), \mathbf{x}(t_2), ..., \mathbf{x}(t_m)]^T$ and the estimated time derivatives $\dot{\mathbf{X}} = [\dot{\mathbf{x}}(t_1), \dot{\mathbf{x}}(t_2), ..., \dot{\mathbf{x}}(t_m)]^T$, we construct a library of candidate functions $\Theta(\mathbf{X}) = [\theta_1(\mathbf{X}), \theta_2(\mathbf{X}), ..., \theta_l(\mathbf{X})]$. We then solve the regression problem, $\dot{\mathbf{X}} = \Theta(\mathbf{X})\Xi$, to identify the optimal functions and coefficients in Θ and Ξ, respectively. A sparsity-promoting regularization function R is typically added to this model discovery problem, yielding the final optimization, $\hat{\Xi} = \arg\min_{\Xi}(\dot{\mathbf{X}} - \Theta(\mathbf{X})\Xi)^2 + R(\Xi)$. Although we focus on this basic implementation, we note that there have been numerous extensions of the original SINDy framework (for a recent overview, see [Kaptanoglu et al., 2022]), many of which can be easily incorporated into the present framework.

Variational Autoencoder The VAE framework [Kingma and Welling, 2014] elegantly integrates variational inference (VI) with deep learning architectures, providing an efficient and powerful approach toward probabilistic modeling. VAEs assume that a set of observations $\mathbf{x}$ derives from a corresponding set of latent states $\mathbf{z}$. VAEs construct an approximate posterior distribution $q_\phi(\mathbf{z}|\mathbf{x})$ and maximize the evidence lower bound (ELBO) of the log likelihood of the data $p_\theta(\mathbf{x})$:

$$\log p_\theta(\mathbf{x}) \geq ELBO(\mathbf{x}, \mathbf{z}) = \mathbb{E}_{q_\phi(\mathbf{z}|\mathbf{x})}[\log p_\theta(\mathbf{x}|\mathbf{z})] - D_{KL}(q_\phi(\mathbf{z}|\mathbf{x})||p_\theta(\mathbf{z})) \tag{2}$$

where ϕ and θ and are the parameters of the inference (encoder) and generative (decoder) models, respectively. The "reparameterization trick" enables sampling from $q_\phi(\mathbf{z}|\mathbf{x})$ using $\mathbf{z} = \mu(\mathbf{z}) + \sigma(\mathbf{z}) \odot \epsilon$ while still training the network end-to-end with backpropagation. After training, new observations are easily generated by sampling from the prior $p_\theta(\mathbf{z})$, typically a unit Gaussian with diagonal covariance.

L_0 Regularization The L_0 norm is ideal for sparse regression problems as it penalizes all nonzero weights equally, regardless of magnitude. As L_0 regularization poses an intractable optimization problem, the L_1 regularization (lasso) – which penalizes the actual values of the learned weights – is a more common technique to achieve sparsity in practice. Nonetheless, incorporation of an L_0-norm penalty [Zheng et al., 2019] into SINDy was recently found to have considerable advantages [Champion et al., 2020], motivating us to adopt a backpropagation-compatible L_0 regularization. Accordingly, we implement one such method recently proposed by Louizos et al. [2018], which penalizes a trainable mask using the hard-concrete distribution.

Specifically, let $M \in \mathbb{R}^d$ be the desired sparse mask. Let s be a binary concrete random variable [Maddison et al., 2017, Jang et al., 2017] distributed in $(0, 1)$ with probability density $q_\phi(s)$, cumulative density $Q_\phi(s)$, location $\log \alpha$, and temperature β. Let $\phi = (\log \alpha, \beta)$. Suppose we have $\gamma < 0$ and $\zeta > 1$. We define each element m in M as a hard concrete random variable computed entirely as a transformation of s. Thus, learning an optimal m necessitates learning $q_\phi(s)$, which simplifies to optimizing $\log \alpha$ (we fix β). Sampling from $q_\phi(s)$ and backpropagating into $\log \alpha$ motivates use of the reparameterization trick (as in the VAE above) with $\epsilon \sim \mathcal{U}(0, 1)$. Then, m is computed.

$$s = \text{Sigmoid}((\log \epsilon - \log(1 - \epsilon) + \log \alpha)/\beta) \qquad m = \min(1, \max(0, s(\zeta - \gamma) + \gamma)) \tag{3}$$

After training, we obtain m using our optimized $\log \alpha$ parameter:

$$m = \min(1, \max(0, \text{Sigmoid}(\log \alpha)(\zeta - \gamma) + \gamma)) \tag{4}$$

We train M using the following loss:

$$L_0(M) = \sum_{j=1}^{d} \text{Sigmoid}(\log \alpha_j - \beta \log \frac{\gamma}{\zeta}) \tag{5}$$

Refer to [Louizos et al., 2018] for the full derivation. In short, this provides a backpropagation-compatible approach to enforce sparsity via a trainable, element-wise mask.

3 HyperSINDy

We combine advances in Bayesian deep learning with the SINDy framework to propose HyperSINDy, a hypernetwork [Ha et al., 2016, Pawlowski et al., 2018] approach to parsimoniously model stochastic nonlinear dynamics via a noise-parameterized vector field whose sparse, time-invariant functional form is discovered from data. In brief, HyperSINDy uses a variational encoder to learn a latent distribution over the states and derivatives of a system, whose posterior is regularized to match a Gaussian prior. Once trained, a white noise process generates a time-varying vector field by updating the coefficients of the discovered (random) ODE. Across a range of experiments, new noise realizations generate stochastic nonlinear dynamics that recapitulate the behavior of the original system, while also enabling UQ on the learned coefficients. Fig. 1 provides an overview of our approach and problem setting, which we detail below.

Problem Setting Stochastic equations are fundamental tools for mathematically modeling dynamics under uncertainty. In general, the precise physical source of uncertainty is unknown and/or of secondary importance [Friedrich et al., 2011, Duan, 2015, Särkkä and Solin, 2019]; as such, several formulations exist. A common choice is the Langevin-type SDE with explicitly separated deterministic (drift) and stochastic (diffusion) terms. Alternatively, we may consider a deterministic ODE with stochastic parameters, i.e., a *random* ODE (RDE), which is another well-established framework [Arnold, 1998, Duan, 2015] with wide-ranging real-world applications (e.g., fluctuating resources in biological systems [Kloeden and Pötzsche, 2013, Caraballo and Han, 2016]). Here, we adopt the RDE formulation in the widely studied setting of i.i.d. noise [Arnold, 1998, Caraballo and Han, 2016]. We find this formulation practically advantageous for integration with deep generative modeling and VI, enabling a powerful and scalable approach to stochastic dynamics. Importantly, as any (finite-dimensional) SDE can be transformed into an equivalent RDE and vice versa [Han and Kloeden, 2017]; these practical advantages can be exploited without compromising relevance to canonical SDE representations (as we will empirically demonstrate).

As above, let $\mathbf{x}_{0:T}$ be the observations from times 0 to T of the state of a system, $\mathbf{x}_t \in \mathbb{R}^n$. We assume these data are generated from some stochastic dynamics $\dot{\mathbf{x}} = f_{\mathbf{z}}(\mathbf{x}_t)$, where $\mathbf{z}$ is a latent random variable to modeled as an i.i.d. noise process. We wish to identify a family of sparse vector field functions $f_{\mathbf{z}}$ constrained to a common functional form for all $\mathbf{z} \in \mathbb{R}^d$ (i.e., only the coefficients of f are time-varying, reflecting the system's dependence on fluctuating quantities).

With this framing, we seek to approximate both the functional form $f_{\mathbf{z}}$ and a posterior estimate of the latent noise trajectory $\mathbf{z} = [\mathbf{z}_0, \mathbf{z}_1, ..., \mathbf{z}_T]^T$ associated with each observed trajectory $\mathbf{x_{0:T}}$. To do so, we employ a variational encoder to learn an inference model for the latent space $p(\mathbf{z}|\mathbf{x}, \dot{\mathbf{x}})$ and a generative model $p(\dot{\mathbf{x}}|\mathbf{x}, \mathbf{z})$ subject to $\dot{\mathbf{x}} = f_{\mathbf{z}}(\mathbf{x})$, as detailed below. Ultimately, once trained, we may generate new trajectories of $\mathbf{x}$ simply by iteratively sampling $\mathbf{z}$ from its Gaussian prior (i.e., constructing new sample paths of the driving noise).

Generative Model Consider the following factorization of the conditional generative model with parameters θ:

$$p_\theta(\dot{\mathbf{x}}, \mathbf{z}|\mathbf{x}) = p_\theta(\dot{\mathbf{x}}|\mathbf{z}, \mathbf{x}) p_\theta(\mathbf{z}) \tag{6}$$

We assume that $\mathbf{z}$ is independent of $\mathbf{x}$, so $p_\theta(\mathbf{z}|\mathbf{x}) = p_\theta(\mathbf{z})$. $p_\theta(\dot{\mathbf{x}}|\mathbf{z}, \mathbf{x})$ describes how the state $\mathbf{x}$ and latent $\mathbf{z}$ are transformed into the derivative, while $p_\theta(\mathbf{z})$ is a prior over the latent distribution of states and their derivatives. We choose $p_\theta(\mathbf{z})$ to be a standard Gaussian with diagonal covariance: $p_\theta(\mathbf{z}) = \mathcal{N}(0, \mathbf{I})$. There are numerous ways to implement $f_\mathbf{z}(\mathbf{x})$, which parameterizes $p_\theta(\dot{\mathbf{x}}|\mathbf{z}, \mathbf{x})$. Following the SINDy framework, which seeks interpretable models in the form of sparse governing equations, we adapt 1 to arrive at the following implementation for $f_\mathbf{z}(\mathbf{x})$:

$$f_\mathbf{z}(\mathbf{x}) = \Theta(\mathbf{x})(\Xi_\mathbf{z} \odot M). \tag{7}$$

where $\odot$ indicates an element-wise multiplication. $\Theta(\mathbf{x})$ is a matrix expansion of $\mathbf{x}$ using a pre-defined library of basis functions, which can include any rational functions, such as polynomial (e.g., $\mathbf{x}_1^2, \mathbf{x}_1\mathbf{x}_2$) or trigonometric (e.g., $\sin \mathbf{x_1}, \tanh \mathbf{x_3}$) functions. $\Xi_\mathbf{z}$ is a matrix of coefficients that is output by a hypernetwork H that takes in $\mathbf{z}$ as input: $\Xi_\mathbf{z} = H(\mathbf{z})$. M is a matrix of values $M_{ij} \in [0, 1]$ that is trained with a close approximation to a differentiable L_0 norm. Specifically, the values of M are simulated using a hard concrete distribution. As such, M enforces sparsity in the terms of each equation through the element-wise multiplication ($\Xi_\mathbf{z} \odot M$). Refer to to the Background section for more details on M.

We constrain $f_\mathbf{z}$ to a d-parameter family of ODEs sharing a common functional form. Specifically, H implements an implicit distribution $p_\theta(\boldsymbol{\Xi}|\mathbf{z})$ with $\mathbf{z} \in \mathbb{R}^d$. Although we cannot compute the density of $p_\theta(\boldsymbol{\Xi}|\mathbf{z})$ exactly, we can generate an ensemble of possible derivative functions by feeding samples $\mathbf{z} \sim p_\theta(\mathbf{z})$ into the hypernetwork: $\Xi_\mathbf{z} = \psi(\mathbf{z})$.

Inference Model Our inference model is defined by the approximate posterior, $q_\phi(\mathbf{z}|\mathbf{x}, \dot{\mathbf{x}})$, with parameters ϕ. $q_\phi(\mathbf{z}|\mathbf{x}, \dot{\mathbf{x}})$ is implemented by a neural network E and the reparameterization trick, i.e., $\mu_q, \sigma_q = E(\mathbf{x}, \dot{\mathbf{x}})$; $\hat{\mathbf{z}} = \mu_q + \epsilon \odot \sigma_q$.

Training We train the model end-to-end with backpropagation to minimize the following loss function:

$$loss = (\dot{\mathbf{x}} - f_{\hat{\mathbf{z}}}(\mathbf{x}))^2 + \beta D_{KL}(q_\phi(\mathbf{z}|\mathbf{x}, \dot{\mathbf{x}})||p_\theta(\mathbf{z})) + \lambda L_0(M) \tag{8}$$

where β and λ are hyperparameters. The loss function optimizes the parameters ϕ and θ, where ϕ are the parameters of E (i.e., the variational parameters) and θ are the parameters of H and M (note that $p_\theta(\mathbf{z})$ has fixed parameters). Refer to the Appendix for a full derivation of this loss function, and to Background for details on the sparsity-related loss $L_0(M)$ (especially equation 5). To speed up training, every set number of epochs, we permanently set values of M equal to 0 if the magnitude of corresponding coefficients fall below a specific threshold value.

4 Results

We evaluate the performance of HyperSINDy on four stochastic dynamical systems. Across a range of (dynamical) noise levels, we seek to assess the accuracy of models identified by HyperSINDy and the degree to which uncertainty estimates faithfully reflect the level of simulated noise. Refer to the Appendix for full details on data generation, training, and simulations.

4.1 Stochastic Equation Discovery

First, we show results for 3D Stochastic Lorenz and 3D Stochastic Rössler datasets, simulated by:

$$\dot{x} = \omega(y - x) \qquad \dot{y} = x(\rho - z) - y \qquad \dot{z} = xy - \beta z \qquad \text{Lorenz} \tag{9}$$

$$\dot{x} = -y - z \qquad \dot{y} = x + ay \qquad \dot{z} = b + z(x - c) \qquad \text{Rössler} \tag{10}$$

where (ω, ρ, β) and (a, b, c) are iteratively sampled (at each timestep) from normal distributions with scale σ and mean $(10, 28, \frac{8}{3})$ and $(0.2, 0.2, 5.7)$, respectively. We train a HyperSINDy model on three trajectories from each system, with $\sigma = 1, 5, 10$. Refer to figure 2 for the full results.

HyperSINDy correctly identifies most terms in each equation. Notably, increasing noise has little impact on the mean coefficients learned by HyperSINDy; instead, the estimated standard deviations of these coefficients proportionately scale with the dynamical noise. Furthermore, HyperSINDy correctly identifies which dynamical terms contain more noise and only increases the standard deviation of those terms, while maintaining tight bounds on other terms (i.e. xy in $\dot{y}$ for Lorenz). Moreover, HyperSINDy is able to simulate the original (stochastic) dynamical behavior even as the noise level increases (blue trajectories). On the other hand, because HyperSINDy also successfully identifies the deterministic functional form despite process noise, it is able to produce smooth trajectories (purple) by forecasting with the mean of the discovered equation ensemble.

Moreover, we ran separate experiments generating 10 trajectories (each with a different random seed, and each generated from a different initial condition) for each noise level of both systems. In total, we trained one HyperSINDy model and one E-SINDy model on each trajectory, yielding 30 HyperSINDy models and 30 E-SINDy models. We evaluated the RMSE of the mean and standard deviation of the discovered equations, as compared to ground truth. Refer to Table 1 for the full results. HyperSINDy outperforms E-SINDy on both mean and standard deviation for each experiment.

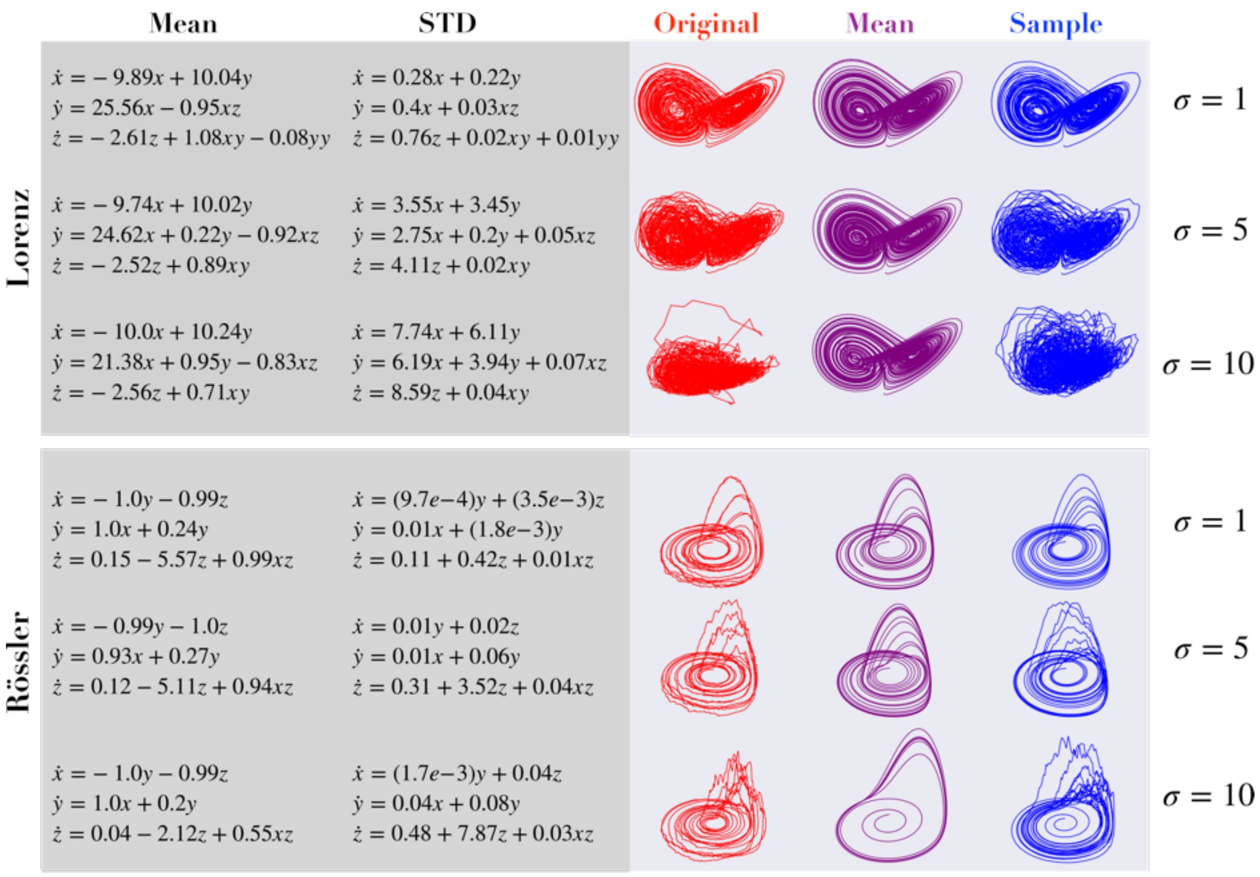

Figure 2: **3D Stochastic Lorenz and Rossler**. HyperSINDy models trained on trajectories of varying noise (σ). The mean and standard deviation of the discovered governing equation coefficients are shown. Refer to 9 and 10 for the ground truth equations. Red trajectories indicate sample test trajectories simulated with the given σ. Purple trajectories are generated from HyperSINDy using the mean of the discovered governing equations, while blue trajectories are generated by iteratively sampling from HyperSINDy's learned generative model. The test and HyperSINDy trajectories are generated from the same initial condition.

Table 1: Total coefficient RMSE relative to ground truth equations

		Lorenz		Rossler	
Param		HyperSINDy	E-SINDy	HyperSINDy	E-SINDy
1	MEAN	**0.082** ± 0.004	0.18 ± 0.029	**0.029** ± 0.035	0.077 ± 0.04
	STD	**0.598** ± 0.045	1.296 ± 0.083	**0.828** ± 0.059	0.849 ± 0.012
5	MEAN	**0.117** ± 0.022	0.268 ± 0.064	**0.086** ± 0.047	0.296 ± 0.199
	STD	**0.4** ± 0.055	0.971 ± 0.024	**0.807** ± 0.012	0.875 ± 0.023
10	MEAN	**0.203** ± 0.047	0.349 ± 0.103	**0.228** ± 0.138	0.699 ± 0.551
	STD	**0.279** ± 0.085	0.913 ± 0.016	**0.812** ± 0.014	0.875 ± 0.028

4.2 Recovering drift-diffusion dynamics

The preceding analyses validate HyperSINDy's capacity for stochastic equation discovery. As HyperSINDy adopts an RDE modeling strategy (i.e., a noise-parameterized ODE [Arnold, 1998, Han and Kloeden, 2017], rather than an SDE with separable drift and diffusion), validation was demonstrated on RDE-simulated data to enable straightforward comparison with ground truth. Crucially, RDEs are conjugate to SDEs [Han and Kloeden, 2017], so this distinction is not fundamental. Nonetheless, this raises the question of how HyperSINDy learns to represent SDE-simulated dynamics.

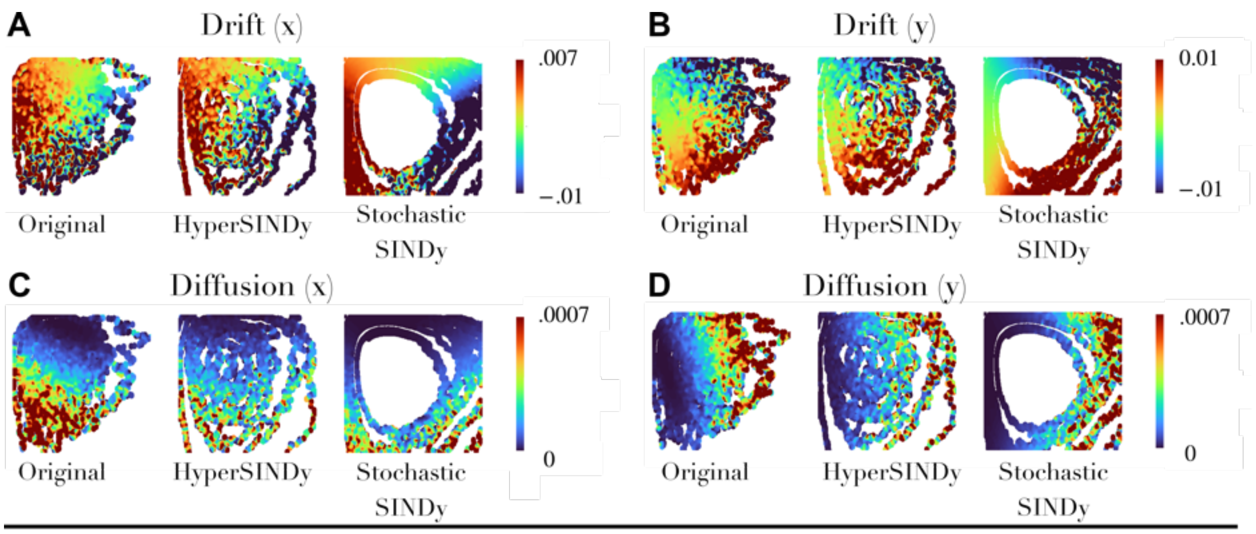

E Equations

Original	HyperSINDy	Stochastic SINDy
Drift	Mean	Drift
$\dot{x} = x - xy$	$\dot{x} = 1.01x - 0.98xy$	$\dot{x} = 0.937x - 0.995xy$
$\dot{y} = -y + xy$	$\dot{y} = -0.97y + 0.99xy$	$\dot{y} = -1.114y + 1.09xy$
Diffusion	STD	Diffusion
$g_{1,1} = 0.25x - 0.09y$	$\dot{x} = 1.63x + 0.25xy$	$g_{1,1} = 0.066x^2 - 0.064xy + 0.019xy^2$
$g_{2,2} = -0.09x + 0.25y$	$\dot{y} = 1.6y + 0.35xy$	$g_{2,2} = 0, -0.037y + 0.071y^2$

Figure 3: **Recovering drift and diffusion behavior in the stochastic Lotka-Volterra model.**. K-M coefficients computed on sample trajectories from each of the three models (Euler-Maruyama integration, $\Delta t = 0.01$). From left to right: the ground truth SDE, the HyperSINDy-discovered system, and the Stochastic SINDy-discovered system.

To address this question, we simulate a 2D SDE to enable direct comparison against the leading method, stochastic SINDy [Boninsegna et al., 2018], as implemented in Python [Nabeel et al., 2022] (which cannot easily scale to higher dimensions). Specifically, we simulate a widely used model for population dynamics, the stochastic Lotka-Volterra system with state-dependent diffusion:

$$\dot{x} = x - xy + \sigma_x(x,y)\mathcal{N}(0,1) \qquad \dot{y} = -y + xy + \sigma_y(x,y)\mathcal{N}(0,1) \tag{11}$$

where we have:

$$\sigma_x(x,y) = 0.25x - 0.09y \qquad \sigma_y(x,y) = -0.09x + 0.25y$$

Figure 3 illustrates the results of this analysis. Notably, HyperSINDy learns an expression whose terms correspond to those of the original drift function, thus enabling physical insight into the system. Moreover, although the diffusion term is not directly comparable with HyperSINDy's representation of stochasticity (coefficient noise), we may numerically estimate drift and diffusion coefficients from HyperSINDy's simulated trajectories. Specifically, we may estimate the first two Kramers-Moyal (K-M) coefficients, which derive from a Taylor expansion of the master equation (and from which derives the Fokker-Planck equation), and which fully describe the Markovian dynamics. Notably, HyperSINDy captures the appropriate deterministic (drift) and stochastic (diffusion) behavior of the system, recapitulating the state-dependence of these terms as seen in the original system – even performing favorably to stochastic SINDy in this setting.

4.3 High Dimensional Stochastic Discovery

Lastly, we assess HyperSINDy's capacity for Bayesian inference/stochastic modeling for high dimensional stochastic systems, which are not amenable to existing analytical SDE discovery methods (e.g., [Boninsegna et al., 2018, Callaham et al., 2021]). Thus, we simulate a stochastic version of the Lorenz-96 system using:

$$\dot{x}_i = F_i + x_{i+1}x_{i-1} - x_{i-2}x_{i-1} - x_i \tag{12}$$

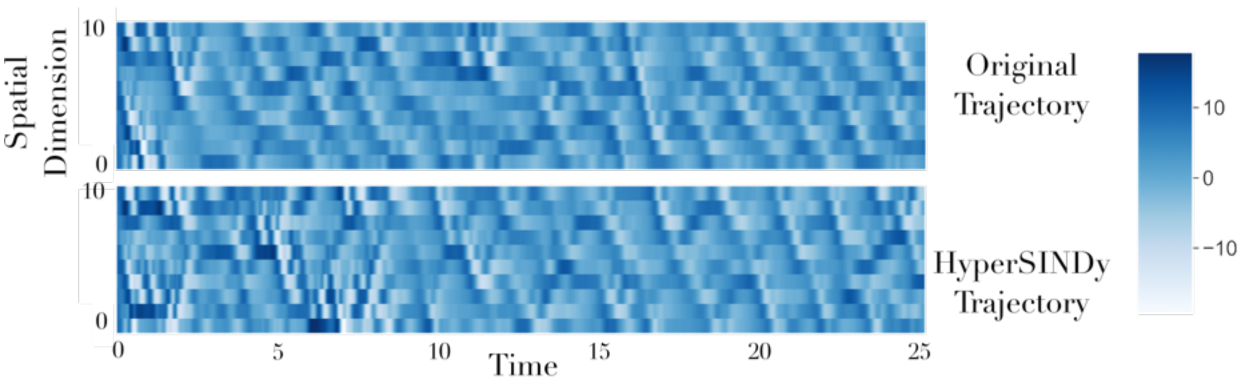

Mean

$$\begin{aligned}
\dot{x}_1 &= 6.75 - 0.75x_1 + 0.99x_2x_{10} - 0.99x_9x_{10}\\
\dot{x}_2 &= 8.46 - 0.74x_2 + 0.98x_1x_3 - 0.99x_1x_{10}\\
\dot{x}_3 &= 7.59 - 0.71x_3 - 0.99x_1x_2 + 0.98x_2x_4\\
\dot{x}_4 &= 7.89 - 0.77x_4 - 0.97x_2x_3 + 0.97x_3x_5\\
\dot{x}_5 &= 6.7 - 0.81x_5 - 0.97x_3x_4 + 0.97x_4x_6\\
\dot{x}_6 &= 7.86 - 0.76x_6 - 0.99x_4x_5 + 0.99x_5x_7\\
\dot{x}_7 &= 7.31 - 0.75x_7 - 0.99x_5x_6 + 0.98x_6x_8\\
\dot{x}_8 &= 7.56 - 0.76x_8 - 0.98x_6x_7 + 0.98x_7x_9\\
\dot{x}_9 &= 7.45 - 0.74x_9 - 0.98x_7x_8 + 0.99x_8x_{10}\\
\dot{x}_{10} &= 6.49 - 0.75x_{10} + 0.99x_1x_9 - 0.99x_8x_9
\end{aligned}$$

STD

$$\begin{aligned}
\dot{x}_1 &= 8.44 + 0.04x_1 + 0.02x_2x_{10} + 0.01x_9x_{10}\\
\dot{x}_2 &= 7.98 + 0.05x_2 + 0.02x_1x_3 + 0.02x_1x_{10}\\
\dot{x}_3 &= 8.1 + 0.05x_3 + 0.01x_1x_2 + 0.02x_2x_4\\
\dot{x}_4 &= 7.72 + 0.04x_4 + 0.01x_2x_3 + 0.01x_3x_5\\
\dot{x}_5 &= 7.65 + 0.04x_5 + 0.02x_3x_4 + 0.01x_4x_6\\
\dot{x}_6 &= 8.47 + 0.05x_6 + 0.03x_4x_5 + 0.01x_5x_7\\
\dot{x}_7 &= 8.09 + 0.06x_7 + 0.01x_5x_6 + 0.02x_6x_8\\
\dot{x}_8 &= 7.89 + 0.03x_8 + 0.02x_6x_7 + 0.01x_7x_9\\
\dot{x}_9 &= 7.97 + 0.04x_9 + 0.01x_7x_8 + 0.02x_8x_{10}\\
\dot{x}_{10} &= 7.83 + 0.03x_{10} + 0.01x_1x_9 + 0.01x_8x_9
\end{aligned}$$

Figure 4: **10D Stochastic Lorenz-96**. A sample test trajectory with $\sigma = 10$ (top) and sample HyperSINDy trajectory (middle) after training on a dataset with $\sigma = 10$. The bottom boxes show the mean and standard deviation of coefficients in the discovered governing equations (cf. 9).

for $i = 1, ..., 10$ where $x_{-1} = x_9$, $x_0 = x_{10}$, and $x_{11} = x_1$. We iteratively sample each F_i from a normal distribution: $F_i \sim \mathcal{N}(8, 10)$. Refer to Fig. 4 for the full results. HyperSINDy correctly identifies all terms in the system, while also correctly learning a high variance coefficient exclusively for the forcing terms, F_i. In addition, HyperSINDy produces sample trajectories that match the stochastic dynamical behavior of ground truth sample trajectories.

5 Discussion

We have provided an overview of HyperSINDy, a neural network-based approach to sparse equation discovery for stochastic dynamics. Importantly, HyperSINDy is unique in its ability to provide analytical representations and UQ in the setting of high-dimensional stochastic dynamics. The present work represents a proof of concept for this architecture. We envision numerous future directions for extending the algorithmic and theoretical aspects of HyperSINDy – e.g., evaluation in the context of other noise types and with respect to convergence in the continuous limit. Moreover, while we employ a fairly straightforward implementation of SINDy, numerous developments of the SINDy framework [Kaptanoglu et al., 2022] may be smoothly incorporated into the HyperSINDy architecture. Finally, the integration of SINDy into a neural network framework paves the way for future developments that incorporate advances in probabilistic machine learning with interpretable equation discovery.

References

L. Arnold. *Random Dynamical Systems*. Springer Monographs in Mathematics. Springer, Berlin, Heidelberg, 1998. ISBN 978-3-642-08355-6 978-3-662-12878-7. doi: 10.1007/978-3-662-12878-7. URL http://link.springer.com/10.1007/978-3-662-12878-7.

L. Boninsegna, F. Nüske, and C. Clementi. Sparse learning of stochastic dynamical equations. *The Journal of Chemical Physics*, 148(24):241723, Mar. 2018. ISSN 0021-9606. doi: 10.1063/1.5018409. URL https://doi.org/10.1063/1.5018409.

S. L. Brunton, J. L. Proctor, and J. N. Kutz. Discovering governing equations from data by sparse identification of nonlinear dynamical systems. *Proceedings of the National Academy of Sciences*, 113(15):3932–3937, Apr. 2016. ISSN 0027-8424, 1091-6490. doi: 10.1073/pnas.1517384113. URL https://pnas.org/doi/full/10.1073/pnas.1517384113.

J. L. Callaham, J.-C. Loiseau, G. Rigas, and S. L. Brunton. Nonlinear stochastic modelling with Langevin regression. *Proceedings of the Royal Society A: Mathematical, Physical and Engineering Sciences*, 477(2250):20210092, June 2021. ISSN 1364-5021, 1471-2946. doi: 10.1098/rspa.2021.0092. URL https://royalsocietypublishing.org/doi/10.1098/rspa.2021.0092.

T. Caraballo and X. Han. *Applied Nonautonomous and Random Dynamical Systems*. SpringerBriefs in Mathematics. Springer International Publishing, Cham, 2016. ISBN 978-3-319-49246-9 978-3-319-49247-6. doi: 10.1007/978-3-319-49247-6. URL http://link.springer.com/10.1007/978-3-319-49247-6.

L. Castrejon, N. Ballas, and A. Courville. Improved Conditional VRNNs for Video Prediction. pages 7608–7617, 2019. URL https://openaccess.thecvf.com/content_ICCV_2019/html/Castrejon_Improved_Conditional_VRNNs_for_Video_Prediction_ICCV_2019_paper.html.

K. Champion, P. Zheng, A. Y. Aravkin, S. L. Brunton, and J. N. Kutz. A Unified Sparse Optimization Framework to Learn Parsimonious Physics-Informed Models From Data. *IEEE Access*, 8:169259–169271, 2020. ISSN 2169-3536. doi: 10.1109/ACCESS.2020.3023625. URL https://ieeexplore.ieee.org/document/9194760/.

J. Duan. *An Introduction to Stochastic Dynamics*. Cambridge University Press, New York, NY, 1st edition edition, Apr. 2015. ISBN 978-1-107-42820-1.

U. Fasel, J. N. Kutz, B. W. Brunton, and S. L. Brunton. Ensemble-SINDy: Robust sparse model discovery in the low-data, high-noise limit, with active learning and control. *Proceedings of the Royal Society A: Mathematical, Physical and Engineering Sciences*, 478(2260):20210904, Apr. 2022. doi: 10.1098/rspa.2021.0904. URL https://royalsocietypublishing.org/doi/10.1098/rspa.2021.0904. Publisher: Royal Society.

R. Friedrich, J. Peinke, M. Sahimi, and M. Reza Rahimi Tabar. Approaching complexity by stochastic methods: From biological systems to turbulence. *Physics Reports*, 506(5):87–162, Sept. 2011. ISSN 03701573. doi: 10.1016/j.physrep.2011.05.003. URL https://linkinghub.elsevier.com/retrieve/pii/S0370157311001530.

A. Ganguly, S. Jain, and U. Watchareeruetai. Amortized Variational Inference: Towards the Mathematical Foundation and Review, Sept. 2022. URL http://arxiv.org/abs/2209.10888. arXiv:2209.10888 [cs, math, stat].

L. M. Gao, U. Fasel, S. L. Brunton, and J. N. Kutz. Convergence of uncertainty estimates in Ensemble and Bayesian sparse model discovery, Jan. 2023. URL http://arxiv.org/abs/2301.12649. arXiv:2301.12649 [cs, math, stat].

C. A. García, P. Félix, J. M. Presedo, and A. Otero. Stochastic embeddings of dynamical phenomena through variational autoencoders. *Journal of Computational Physics*, 454:110970, Apr. 2022. ISSN 0021-9991. doi: 10.1016/j.jcp.2022.110970. URL https://www.sciencedirect.com/science/article/pii/S0021999122000328.

L. Girin, S. Leglaive, X. Bie, J. Diard, T. Hueber, and X. Alameda-Pineda. Dynamical Variational Autoencoders: A Comprehensive Review. *Foundations and Trends® in Machine Learning*, 15(1-2):1–175, Dec. 2021. ISSN 1935-8237, 1935-8245. doi: 10.1561/2200000089. URL https://www.nowpublishers.com/article/Details/MAL-089. Publisher: Now Publishers, Inc.

D. Ha, A. Dai, and Q. V. Le. HyperNetworks, Dec. 2016. URL http://arxiv.org/abs/1609.09106. arXiv:1609.09106 [cs].

X. Han and P. E. Kloeden. *Random Ordinary Differential Equations and Their Numerical Solution*, volume 85 of *Probability Theory and Stochastic Modelling*. Springer Singapore, Singapore, 2017. ISBN 978-981-10-6264-3 978-981-10-6265-0. doi: 10.1007/978-981-10-6265-0. URL http://link.springer.com/10.1007/978-981-10-6265-0.

A. Hasan, J. M. Pereira, S. Farsiu, and V. Tarokh. Identifying Latent Stochastic Differential Equations. *IEEE Transactions on Signal Processing*, 70:89–104, 2022. ISSN 1941-0476. doi: 10.1109/TSP.2021.3131723. Conference Name: IEEE Transactions on Signal Processing.

S. M. Hirsh, D. A. Barajas-Solano, and J. N. Kutz. Sparsifying Priors for Bayesian Uncertainty Quantification in Model Discovery, July 2021. URL http://arxiv.org/abs/2107.02107. arXiv:2107.02107 [math].

Y. Huang, Y. Mabrouk, G. Gompper, and B. Sabass. Sparse inference and active learning of stochastic differential equations from data. *Scientific Reports*, 12(1):21691, Dec. 2022. ISSN 2045-2322. doi: 10.1038/s41598-022-25638-9. URL https://www.nature.com/articles/s41598-022-25638-9. Number: 1 Publisher: Nature Publishing Group.

E. Jang, S. Gu, and B. Poole. Categorical Reparameterization with Gumbel-Softmax, Aug. 2017. URL http://arxiv.org/abs/1611.01144. arXiv:1611.01144 [cs, stat].

A. A. Kaptanoglu, B. M. d. Silva, U. Fasel, K. Kaheman, A. J. Goldschmidt, J. Callaham, C. B. Delahunt, Z. G. Nicolaou, K. Champion, J.-C. Loiseau, J. N. Kutz, and S. L. Brunton. PySINDy: A comprehensive Python package for robust sparse system identification. *Journal of Open Source Software*, 7(69):3994, Jan. 2022. ISSN 2475-9066. doi: 10.21105/joss.03994. URL https://joss.theoj.org/papers/10.21105/joss.03994.

G. E. Karniadakis, I. G. Kevrekidis, L. Lu, P. Perdikaris, S. Wang, and L. Yang. Physics-informed machine learning. *Nature Reviews Physics*, 3(6):422–440, June 2021. ISSN 2522-5820. doi: 10.1038/s42254-021-00314-5. URL https://www.nature.com/articles/s42254-021-00314-5. Number: 6 Publisher: Nature Publishing Group.

D. P. Kingma and M. Welling. Auto-Encoding Variational Bayes, May 2014. URL http://arxiv.org/abs/1312.6114. arXiv:1312.6114 [cs, stat].

D. P. Kingma and M. Welling. An Introduction to Variational Autoencoders. *Foundations and Trends® in Machine Learning*, 12(4):307–392, Nov. 2019. ISSN 1935-8237, 1935-8245. doi: 10.1561/2200000056. URL https://www.nowpublishers.com/article/Details/MAL-056. Publisher: Now Publishers, Inc.

P. E. Kloeden and C. Pötzsche, editors. *Nonautonomous Dynamical Systems in the Life Sciences*, volume 2102 of *Lecture Notes in Mathematics*. Springer International Publishing, Cham, 2013. ISBN 978-3-319-03079-1 978-3-319-03080-7. doi: 10.1007/978-3-319-03080-7. URL https://link.springer.com/10.1007/978-3-319-03080-7.

B. Lim and S. Zohren. Time-series forecasting with deep learning: a survey. *Philosophical Transactions of the Royal Society A: Mathematical, Physical and Engineering Sciences*, 379(2194):20200209, Feb. 2021. doi: 10.1098/rsta.2020.0209. URL https://royalsocietypublishing.org/doi/full/10.1098/rsta.2020.0209. Publisher: Royal Society.

R. Lopez and P. J. Atzberger. Variational Autoencoders for Learning Nonlinear Dynamics of Physical Systems, Mar. 2021. URL http://arxiv.org/abs/2012.03448. arXiv:2012.03448 [cs, eess, math].

I. Loshchilov and F. Hutter. Decoupled Weight Decay Regularization, Jan. 2019. URL http://arxiv.org/abs/1711.05101. arXiv:1711.05101 [cs, math].

C. Louizos, M. Welling, and D. P. Kingma. Learning Sparse Neural Networks through \$L_0\$ Regularization, June 2018. URL http://arxiv.org/abs/1712.01312. arXiv:1712.01312 [cs, stat].

C. J. Maddison, A. Mnih, and Y. W. Teh. The Concrete Distribution: A Continuous Relaxation of Discrete Random Variables, Mar. 2017. URL http://arxiv.org/abs/1611.00712. arXiv:1611.00712 [cs, stat].

D. A. Messenger and D. M. Bortz. Weak SINDy: Galerkin-Based Data-Driven Model Selection. *Multiscale Modeling & Simulation*, 19(3):1474–1497, Jan. 2021. ISSN 1540-3459, 1540-3467. doi: 10.1137/20M1343166. URL http://arxiv.org/abs/2005.04339. arXiv:2005.04339 [cs, math].

A. Nabeel, A. Karichannavar, S. Palathingal, J. Jhawar, D. R. M, and V. Guttal. PyDaddy: A Python package for discovering stochastic dynamical equations from timeseries data, Nov. 2022. URL http://arxiv.org/abs/2205.02645. arXiv:2205.02645 [cs, math, q-bio].

R. Nayek, R. Fuentes, K. Worden, and E. J. Cross. On spike-and-slab priors for Bayesian equation discovery of nonlinear dynamical systems via sparse linear regression. *Mechanical Systems and Signal Processing*, 161:107986, Dec. 2021. ISSN 0888-3270. doi: 10.1016/j.ymssp.2021.107986. URL https://www.sciencedirect.com/science/article/pii/S0888327021003812.

D. Nguyen, S. Ouala, L. Drumetz, and R. Fablet. Variational Deep Learning for the Identification and Reconstruction of Chaotic and Stochastic Dynamical Systems from Noisy and Partial Observations, Feb. 2021. URL http://arxiv.org/abs/2009.02296. arXiv:2009.02296 [cs, stat].

R. K. Niven, A. Mohammad-Djafari, L. Cordier, M. Abel, and M. Quade. Bayesian Identification of Dynamical Systems. *Proceedings*, 33(1):33, 2020. ISSN 2504-3900. doi: 10.3390/proceedings2019033033. URL https://www.mdpi.com/2504-3900/33/1/33. Number: 1 Publisher: Multidisciplinary Digital Publishing Institute.

A. Paszke, S. Gross, F. Massa, A. Lerer, J. Bradbury, G. Chanan, T. Killeen, Z. Lin, N. Gimelshein, L. Antiga, A. Desmaison, A. Kopf, E. Yang, Z. DeVito, M. Raison, A. Tejani, S. Chilamkurthy, B. Steiner, L. Fang, J. Bai, and S. Chintala. PyTorch: An Imperative Style, High-Performance Deep Learning Library. In *Advances in Neural Information Processing Systems*, volume 32. Curran Associates, Inc., 2019. URL `https://proceedings.neurips.cc/paper/2019/hash/bdbca288fee7f92f2bfa9f7012727740-Abstract.html`.

N. Pawlowski, A. Brock, M. C. H. Lee, M. Rajchl, and B. Glocker. Implicit Weight Uncertainty in Neural Networks, May 2018. URL `http://arxiv.org/abs/1711.01297`. arXiv:1711.01297 [cs, stat].

S. J. Reddi, S. Kale, and S. Kumar. On the Convergence of Adam and Beyond, Apr. 2019. URL `http://arxiv.org/abs/1904.09237`. arXiv:1904.09237 [cs, math, stat].

D. Rezende and S. Mohamed. Variational Inference with Normalizing Flows. In *Proceedings of the 32nd International Conference on Machine Learning*, pages 1530–1538. PMLR, June 2015. URL `https://proceedings.mlr.press/v37/rezende15.html`. ISSN: 1938-7228.

M. Schmidt and H. Lipson. Distilling Free-Form Natural Laws from Experimental Data. *Science*, 324(5923):81–85, Apr. 2009. ISSN 0036-8075, 1095-9203. doi: 10.1126/science.1165893. URL `https://www.science.org/doi/10.1126/science.1165893`.

L. Sun, H. Sun, D. Z. Huang, and J.-X. Wang. Bayesian Spline Learning for Equation Discovery of Nonlinear Dynamics with Quantified Uncertainty.

S. Särkkä and A. Solin. *Applied Stochastic Differential Equations*. Cambridge University Press, 1 edition, Apr. 2019. ISBN 978-1-108-18673-5 978-1-316-51008-7 978-1-316-64946-6. doi: 10.1017/9781108186735. URL `https://www.cambridge.org/core/product/identifier/9781108186735/type/book`.

N. Takeishi and A. Kalousis. Physics-Integrated Variational Autoencoders for Robust and Interpretable Generative Modeling. In *Advances in Neural Information Processing Systems*, volume 34, pages 14809–14821. Curran Associates, Inc., 2021. URL `https://proceedings.neurips.cc/paper/2021/hash/7ca57a9f85a19a6e4b9a248c1daca185-Abstract.html`.

T. Tripura and S. Chakraborty. A sparse Bayesian framework for discovering interpretable nonlinear stochastic dynamical systems with Gaussian white noise. *Mechanical Systems and Signal Processing*, 187:109939, Mar. 2023. ISSN 0888-3270. doi: 10.1016/j.ymssp.2022.109939. URL `https://www.sciencedirect.com/science/article/pii/S088832702201007X`.

Y. Wang, H. Fang, J. Jin, G. Ma, X. He, X. Dai, Z. Yue, C. Cheng, H.-T. Zhang, D. Pu, D. Wu, Y. Yuan, J. Gonçalves, J. Kurths, and H. Ding. Data-Driven Discovery of Stochastic Differential Equations. *Engineering*, 17:244–252, Oct. 2022. ISSN 2095-8099. doi: 10.1016/j.eng.2022.02.007. URL `https://www.sciencedirect.com/science/article/pii/S209580992200145X`.

Y. Yacoby, W. Pan, and F. Doshi-Velez. Failure Modes of Variational Autoencoders and Their Effects on Downstream Tasks, Mar. 2022. URL `http://arxiv.org/abs/2007.07124`. arXiv:2007.07124 [cs, stat].

L. Yang, D. Zhang, and G. E. Karniadakis. Physics-Informed Generative Adversarial Networks for Stochastic Differential Equations. *SIAM Journal on Scientific Computing*, 42(1):A292–A317, Jan. 2020. ISSN 1064-8275. doi: 10.1137/18M1225409. URL `https://epubs.siam.org/doi/10.1137/18M1225409`. Publisher: Society for Industrial and Applied Mathematics.

J. Yoon, D. Jarrett, and M. van der Schaar. Time-series Generative Adversarial Networks. In *Advances in Neural Information Processing Systems*, volume 32. Curran Associates, Inc., 2019. URL `https://papers.nips.cc/paper_files/paper/2019/hash/c9efe5f26cd17ba6216bbe2a7d26d490-Abstract.html`.

D. Zhang, L. Lu, L. Guo, and G. E. Karniadakis. Quantifying total uncertainty in physics-informed neural networks for solving forward and inverse stochastic problems. *Journal of Computational Physics*, 397:108850, Nov. 2019. ISSN 0021-9991. doi: 10.1016/j.jcp.2019.07.048. URL `https://www.sciencedirect.com/science/article/pii/S0021999119305340`.

P. Zheng, T. Askham, S. L. Brunton, J. N. Kutz, and A. Y. Aravkin. A Unified Framework for Sparse Relaxed Regularized Regression: SR3. *IEEE Access*, 7:1404–1423, 2019. ISSN 2169-3536. doi: 10.1109/ACCESS.2018.2886528. Conference Name: IEEE Access.

W. Zhong and H. Meidani. PI-VAE: Physics-Informed Variational Auto-Encoder for stochastic differential equations. *Computer Methods in Applied Mechanics and Engineering*, 403:115664, Jan. 2023. ISSN 0045-7825. doi: 10.1016/j.cma.2022.115664. URL `https://www.sciencedirect.com/science/article/pii/S0045782522006193`.

Appendix A Derivation of Loss Function

We assume independence of $\mathbf{z}$ with respect to $\mathbf{x}$, such that $p_\theta(\mathbf{z}|\mathbf{x}) = p_\theta(\mathbf{z})$. Then, as described in the Methods section, our generative model factorizes as follows (Bayes' rule):

$$p_\theta(\dot{\mathbf{x}}, \mathbf{z}|\mathbf{x}) = p_\theta(\dot{\mathbf{x}}|\mathbf{z}, \mathbf{x}) p_\theta(\mathbf{z}) \tag{13}$$

Given the chain rule for conditional probability, we also have:

$$\begin{aligned} p_\theta(\dot{\mathbf{x}}|\mathbf{z}, \mathbf{x}) &= \frac{p_\theta(\dot{\mathbf{x}}, \mathbf{z}, \mathbf{x})}{p_\theta(\mathbf{z}, \mathbf{x})} && \text{Conditional Probability} \\ &= \frac{p_\theta(\mathbf{z}|\dot{\mathbf{x}}, \mathbf{x}) p_\theta(\dot{\mathbf{x}}|\mathbf{x}) p_\theta(\mathbf{x})}{p_\theta(\mathbf{z}|\mathbf{x}) p_\theta(\mathbf{x})} \\ &= \frac{p_\theta(\mathbf{z}|\dot{\mathbf{x}}, \mathbf{x}) p_\theta(\dot{\mathbf{x}}|\mathbf{x})}{p_\theta(\mathbf{z})} && p_\theta(\mathbf{z}|\mathbf{x}) = p_\theta(\mathbf{z}) \end{aligned}$$

By substituting into the first factorization, we obtain the second factorization:

$$p_\theta(\dot{\mathbf{x}}, \mathbf{z}|\mathbf{x}) = p_\theta(\mathbf{z}|\dot{\mathbf{x}}, \mathbf{x}) p_\theta(\dot{\mathbf{x}}|\mathbf{x}) \tag{14}$$

We seek to learn a model that captures the dynamics $\dot{\mathbf{x}}$, given the state $\mathbf{x}$. Specifically, we seek to maximize the log-likelihood $\log p_\theta(\dot{\mathbf{x}}|\mathbf{x})$ by performing inference over $\mathbf{z}$. We follow a similar derivation as in [Kingma and Welling, 2019]:

$$\begin{aligned} \log p_\theta(\dot{\mathbf{x}}|\mathbf{x}) &= \mathbb{E}_{q_\phi(\mathbf{z}|\dot{\mathbf{x}}, \mathbf{x})}\left[\log p_\theta(\dot{\mathbf{x}}|\mathbf{x})\right] \\ &= \mathbb{E}_{q_\phi(\mathbf{z}|\dot{\mathbf{x}}, \mathbf{x})}\left[\log \frac{p_\theta(\dot{\mathbf{x}}, \mathbf{z}|\mathbf{x})}{p_\theta(\mathbf{z}|\dot{\mathbf{x}}, \mathbf{x})}\right] && \text{see Eq. 14} \\ &= \mathbb{E}_{q_\phi(\mathbf{z}|\dot{\mathbf{x}}, \mathbf{x})}\left[\log \frac{p_\theta(\dot{\mathbf{x}}, \mathbf{z}|\mathbf{x}) q_\phi(\mathbf{z}|\dot{\mathbf{x}}, \mathbf{x})}{p_\theta(\mathbf{z}|\dot{\mathbf{x}}, \mathbf{x}) q_\phi(\mathbf{z}|\dot{\mathbf{x}}, \mathbf{x})}\right] \\ &= \mathbb{E}_{q_\phi(\mathbf{z}|\dot{\mathbf{x}}, \mathbf{x})}\left[\log \frac{p_\theta(\dot{\mathbf{x}}, \mathbf{z}|\mathbf{x})}{q_\phi(\mathbf{z}|\dot{\mathbf{x}}, \mathbf{x})}\right] + \mathbb{E}_{q_\phi(\mathbf{z}|\dot{\mathbf{x}}, \mathbf{x})}\left[\log \frac{q_\phi(\mathbf{z}|\dot{\mathbf{x}}, \mathbf{x})}{p_\theta(\mathbf{z}|\dot{\mathbf{x}}, \mathbf{x})}\right] \\ &= ELBO + D_{KL}(q_\phi(\mathbf{z}|\dot{\mathbf{x}}, \mathbf{x}) || p_\theta(\mathbf{z}|\dot{\mathbf{x}}, \mathbf{x})) \end{aligned}$$

Since $D_{KL}(q_\phi(\mathbf{z}|\dot{\mathbf{x}}, \mathbf{x}) || p_\theta(\mathbf{z}|\dot{\mathbf{x}}, \mathbf{x})) \geq 0$, we maximize the $ELBO$, which lower bounds $\log p_\theta(\dot{\mathbf{x}}|\mathbf{x})$.

$$\begin{aligned} ELBO &= \mathbb{E}_{q_\phi(\mathbf{z}|\dot{\mathbf{x}}, \mathbf{x})}\left[\log \frac{p_\theta(\dot{\mathbf{x}}, \mathbf{z}|\mathbf{x})}{q_\phi(\mathbf{z}|\dot{\mathbf{x}}, \mathbf{x})}\right] \\ &= \mathbb{E}_{q_\phi(\mathbf{z}|\dot{\mathbf{x}}, \mathbf{x})}\left[\log p_\theta(\dot{\mathbf{x}}, \mathbf{z}|\mathbf{x}) - \log q_\phi(\mathbf{z}|\dot{\mathbf{x}}, \mathbf{x})\right] \\ &= \mathbb{E}_{q_\phi(\mathbf{z}|\dot{\mathbf{x}}, \mathbf{x})}\left[\log p_\theta(\dot{\mathbf{x}}|\mathbf{z}, \mathbf{x}) + \log p_\theta(\mathbf{z}) - \log q_\phi(\mathbf{z}|\dot{\mathbf{x}}, \mathbf{x})\right] && \text{see Eq. 13} \\ &= \mathbb{E}_{q_\phi(\mathbf{z}|\dot{\mathbf{x}}, \mathbf{x})}\left[\log p_\theta(\dot{\mathbf{x}}|\mathbf{z}, \mathbf{x}) - D_{KL}(q_\phi(\mathbf{z}|\dot{\mathbf{x}}, \mathbf{x}) || p_\theta(\mathbf{z}))\right] \end{aligned}$$

Equivalently, we can minimize the $-ELBO$, given by the following loss:

$$loss = (\dot{\mathbf{x}} - f_{\hat{\mathbf{z}}}(\mathbf{x}))^2 + D_{KL}(q_\phi(\mathbf{z}|\mathbf{x}, \dot{\mathbf{x}}) || p_\theta(\mathbf{z}))$$

Given our goal to learn a sparse set of governing equations, we need to train M, which is multiplied elementwise with Ξ_z. To do so, we add $L_0(M)$ (main text Eq. 5) to the loss, yielding:

$$\begin{aligned} loss &= (\dot{\mathbf{x}} - f_{\hat{\mathbf{z}}}(\mathbf{x}))^2 + \beta D_{KL}(q_\phi(\mathbf{z}|\mathbf{x}, \dot{\mathbf{x}}) || p_\theta(\mathbf{z})) + \lambda L_0(M) \\ &= (\dot{\mathbf{x}} - f_{\hat{\mathbf{z}}}(\mathbf{x}))^2 + \beta D_{KL}(q_\phi(\mathbf{z}|\mathbf{x}, \dot{\mathbf{x}}) || p_\theta(\mathbf{z})) + \lambda \sum_{j=1}^{k} \text{Sigmoid}(\log \alpha_j - \beta_{L_0} \log \frac{\gamma}{\zeta}) \end{aligned}$$

where β, λ, β_{L_0}, γ, and ζ are hyperparameters, k is the dimension of a vectorized M, and $\hat{\mathbf{z}} \sim q_\phi(\mathbf{z}|\mathbf{x}, \dot{\mathbf{x}})$ using the reparameterization trick. $log\alpha_j$ are location parameters for the distribution that M is transformed from, as described in the Background section of the main text.

Table 2: Matrix shapes for different experiments

System	n	C	$\Theta(x)$	Ξ_z	M	$\Theta(x)(\Xi_z \odot M)$
Lorenz	3	F	250×19	$250 \times 19 \times 3$	$250 \times 19 \times 3$	250×3
Rössler	3	T	250×20	$250 \times 20 \times 3$	$250 \times 20 \times 3$	250×3
Lotka-Volterra	2	T	250×10	$250 \times 10 \times 2$	$250 \times 10 \times 2$	250×2
Lorenz-96	10	T	250×286	$250 \times 286 \times 10$	$250 \times 286 \times 10$	250×10

Table 3: Dataset initial conditions

System	Train	Test
Lorenz	(0, 1, 1.05)	(-1, 2, 0.5)
Rössler	(0, 1, 1.05)	(-1, 2, 0.5)
Lotka-Volterra	(4, 2)	(2.1, 1.0)
Lorenz-96	(8.01, 8, 8, 8, 8, 8, 8, 8, 8, 8)	(7.8, 8.7, 8.5, 6.0, 9.9, 9.5, 7.5, 6.9, 6.9, 8.7)

Appendix B Generative and Inference Models

Matrix dimensions are variable. Consider $x \in \mathbb{R}^n$ and a library with l terms. Then, we have:

$$\Theta(x) \in \mathbb{R}^l \qquad \Xi_z \in \mathbb{R}^{l \times n} \qquad M \in \mathbb{R}^{l \times n} \qquad (\Xi_z \odot M) \in \mathbb{R}^{l \times n} \qquad \Theta(x)(\Xi_z \odot M) \in \mathbb{R}^n$$

However, we use minibatches during training. Consider a batch of x of size b, meaning $x \in \mathbb{R}^{b \times n}$. Then, we have:

$$\Theta(x) \in \mathbb{R}^{b \times l} \qquad \Xi_z \in \mathbb{R}^{b \times l \times n} \qquad M \in \mathbb{R}^{b \times l \times n} \qquad (\Xi_z \odot M) \in \mathbb{R}^{b \times l \times n} \qquad \Theta(x)(\Xi_z \odot M) \in \mathbb{R}^{b \times n}$$

After training, we do not sample M using the reparameterization trick, since α has been learned. So, M has shape $l \times n$ (note that $k = l \cdot n$). For all experiments, we included polynomials up to order 3 in the library and used a batch size of 250 during training. Refer to Table 2 for a breakdown of matrix shapes for each experiment during training (note that C refers to whether a constant is included in the library).

Appendix C Data

Each trajectory was generated for 10000 timesteps with $dt = 0.01$. Refer to Table 3 for data generation initial conditions. Note that the test initial condition for Lorenz-96 is rounded (the exact values can be found in the accompanying code, as we used Gaussian noise to choose the initial condition). Derivatives are estimated using finite differences without smoothing.

Appendix D Training

D.1 Algorithm

A "best practice" for the HyperSINDy training algorithm is choosing low initial β and λ values and evaluating the results before adjusting in future runs. Moreover, we also utilize beta warmup Castrejon et al. [2019], which is useful for avoiding posterior collapse in VAEs. Specifically, we increase the β value from 0.01 to the chosen low initial β value over 100 epochs. If the prior did not learn the function well enough, we increased ("spiked") the β value at a later epoch in training to β_{spike}. Note that, although we knew the ground truth coefficients in our simulations, one can determine whether the prior learned "well enough" by comparing the similarity between the coefficients generated from the prior to the coefficients generated from the approximate posterior. See [Yacoby et al., 2022] for more information on this tradeoff between the posterior and prior. If the learned model was not sparse enough, we increased the λ value at a later epoch in training to λ_{spike}.

Every 100 epochs, we permanently set values in M to be zero if the corresponding coefficients (using the mean over a batch of coefficients) falls below the threshold value T. This is done using an auxiliary matrix of shape $l \times n$, where the values are all initially set to 1 and then set to 0 throughout training if the corresponding value in M should be 0 permanently. This mask is multiplied elementwise with M to enforce this permanent sparsity. During training, we sample one M for each example in a minibatch of data using the reparameterization trick.

Table 4: Hyperparameters

Lorenz							
σ	d	β_{spike}	$epoch_{\beta_{spike}}$	λ_{spike}	$epoch_{\lambda_{spike}}$	$epochs$	T
1	6	100	400	10	400	999	0.05
5	6	400	400	10	400	999	0.05
10	6	400	400	10	400	999	0.05
Rössler							
σ	d	β_{spike}	$epoch_{\beta_{spike}}$	λ_{spike}	$epoch_{\lambda_{spike}}$	$epochs$	T
1	6	100	200	0.1	200	499	0.01
5	6	100	200	0.1	300	600	0.01
10	6	100	200	1	300	600	0.01
Lorenz RMSE							
σ	d	β_{spike}	$epoch_{\beta_{spike}}$	λ_{spike}	$epoch_{\lambda_{spike}}$	$epochs$	T
1	6	100	400	10	400	999	0.05
5	6	400	400	10	400	999	0.05
10	6	400	400	10	400	999	0.05
Rössler RMSE							
σ	d	β_{spike}	$epoch_{\beta_{spike}}$	λ_{spike}	$epoch_{\lambda_{spike}}$	$epochs$	T
1	6	100	200	0.1	200	499	0.01
5	6	200	200	0.1	300	600	0.01
10	6	300	200	1	300	600	0.01
Lotka-Volterra							
σ	d	β_{spike}	$epoch_{\beta_{spike}}$	λ_{spike}	$epoch_{\lambda_{spike}}$	$epochs$	T
N/A	4	None	None	0.1	100	250	0.1
Lorenz-96							
σ	d	β_{spike}	$epoch_{\beta_{spike}}$	λ_{spike}	$epoch_{\lambda_{spike}}$	$epochs$	T
10	20	None	None	10	400	999	0.05

D.2 Hyperparameters

Hyperparamater tuning mostly consists of adjusting the β and λ value for the Kl divergence and L_0 terms in the loss function, respectively. Hyperparameters that stay constant for all experiments are listed here: $learning\_rate = 0.005$, $num\_hidden = 5$, $stat\_size = 250$, $batch\_size = 250$. $stat\_size$ refers to the number of coefficient matrices that are sampled from the prior to calculate the coefficient means used for the permanent thresholding described in the Training section. We used a hidden dimension of 64 in all neural networks for all experiments except on Lorenz-96, for which we used a hidden dimension of 128. We warm up to a low initial β value of 10 for every experiment. We use an initial L_0 regularization weight of $\lambda = 0.01$. For M, we use $\beta_{L_0} = 2/3$, $\gamma = -0.1$, and $\zeta = 1.1$. Note that an exhaustive list of hyperparameters and training settings can be found in the accompanying code. All experiments were run on an NVIDIA GeForce RTX 2080 Ti GPU. We ran all experiments in PyTorch [Paszke et al., 2019] using the AdamW optimizer [Loshchilov and Hutter, 2019] with a weight decay value of 0.01 and amsgrad [Reddi et al., 2019] enabled. Refer to Table 4 for a list of hyperparameters that we tuned to obtain the results in the main text. Refer to the attached code for more details on the RMSE experiments, as well as information on settings used to generate the supplemental figures.

Appendix E RMSE Metric

To generate Table 1, we use the RMSE metric (as computed in Sun et al.). Specifically, we compute:

$$rmse = \frac{||\mathbf{C}_{True} - \mathbf{C}_{Pred}||_2}{||\mathbf{C}_{True}||_2}$$

where $\mathbf{C}_{True}$ is the true mean or standard deviatin of a given coefficient, and $\mathbf{C}_{Pred}$ is the mean or standard deviation of the predicted coefficients. For terms that are not included in the ground truth or predicted equations, we consider their mean or standard deviation to be zero.

Appendix F Algorithms

Algorithm 1 Generation of Governing Equations Coefficients, Ξ_z, to predict $\dot{\mathbf{x}}$

```
1: if $\mathbf{z}$ not given then:
2:     $\mathbf{z} \sim \mathcal{N}(0, I)$                          ▷ Generate batch of $\mathbf{z}$
3: $\Xi_{\mathbf{z}} = H(\mathbf{z})$                   ▷ Generate 1 coefficient matrix for each $\mathbf{z}$ in batch
4: $\dot{\mathbf{x}} = f_{\mathbf{z}}(\mathbf{x}) = \Theta(\mathbf{x})(\Xi_{\mathbf{z}} \odot M)$          ▷ Unless training, uses Eq 4 to get M
```

Algorithm 2 Training Loop for Each Epoch

```
1: for each minibatch $\mathbf{x}, \dot{\mathbf{x}}$ do
2:     $\mu_q, \sigma_q = E(\mathbf{x}, \dot{\mathbf{x}})$                      ▷ Encode each element of batch
3:     $\hat{\mathbf{z}} = \mu_q + \sigma_q \odot \epsilon$                        ▷ Reparameterization Trick
4:     Obtain training $M$ through transformations        ▷ See Background, specifically Eq 3
5:     $\hat{\dot{\mathbf{x}}} = f_{\hat{\mathbf{z}}}(\mathbf{x}) =$ Algorithm 1($\hat{\mathbf{z}}$)                 ▷ Give $\hat{\mathbf{z}}$ to H
6:     $loss = (\dot{\mathbf{x}} - \hat{\dot{\mathbf{x}}})^2 + \beta D_{KL}(q_\phi(\mathbf{z}|\mathbf{x}, \dot{\mathbf{x}})||p_\theta(\mathbf{z})) + \lambda L_0(M)$
7:     Backprop $loss$ and update $\theta, \phi$
8: Sample batch of $\mathbf{z} \sim \mathcal{N}(0, 1)$
9: $\Xi_{\mathbf{z}} = H(\mathbf{z})$
10: $\Xi_{\mathbf{z}_{mean}}$ = mean over batch of $\Xi_{\mathbf{z}}$
11: if (epoch $\%$ threshold_interval) == 0 then:          ▷ If we must threshold this epoch
12:     $M = 0$ permanently where $abs(\Xi_{\mathbf{z}_{mean}}) < threshold$   ▷ Permanently threshold M
```

Appendix G Figures

We include here additional sample trajectories (all from the test initial condition) to highlight HyperSINDy's generative capabilities. Refer to Figure 5 for HyperSINDy trajectories generated for various noise levels on the Lorenz and Rössler system, and refer to Figure 6 for sample test trajectories. HyperSINDy captures the same dynamical behavior as the original system. Refer to Figure 7 for HyperSINDy trajectories generated for the Lorenz-96 system.

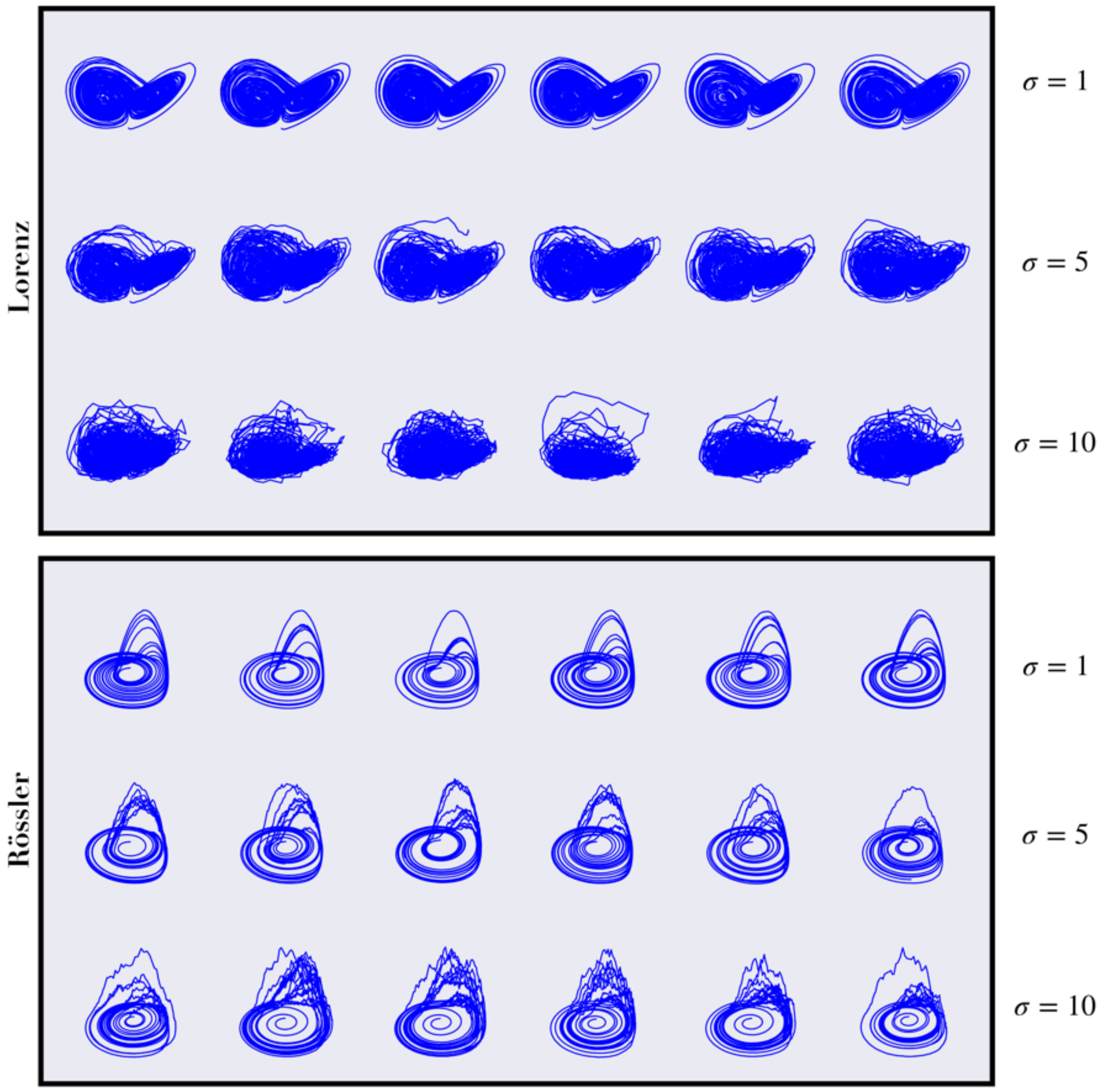

Figure 5: **3D Stochastic Lorenz and Rössler Samples**. HyperSINDy models trained on trajectories of varying noise (σ). Blue trajectories are generated by iteratively sampling from HyperSINDy's learned generative model.

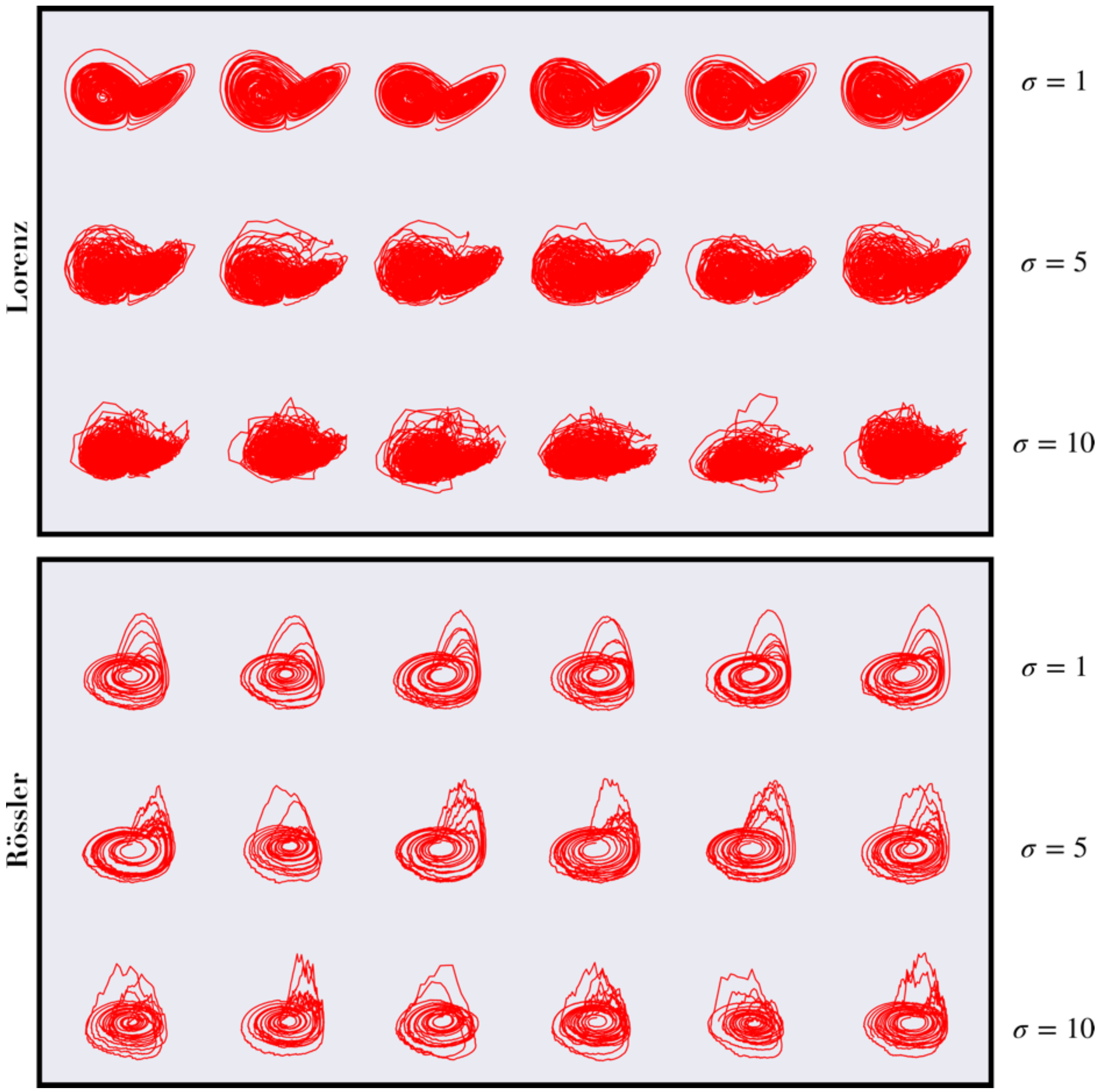

Figure 6: **3D Stochastic Lorenz and Rössler Ground Truth Samples**. Samples generated using the ground truth equations for varying noise levels (σ).

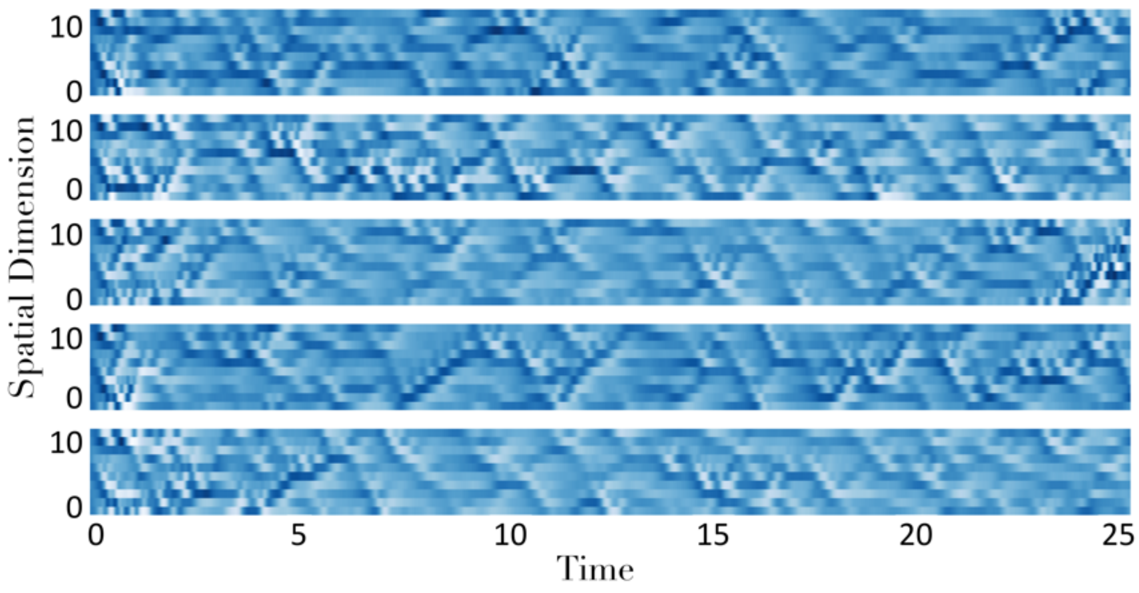

Figure 7: **Lorenz-96 Samples** (σ = 10). Each row contains a different sample trajectory. Trajectories are generated by iteratively sampling from HyperSINDy's learned generative model.

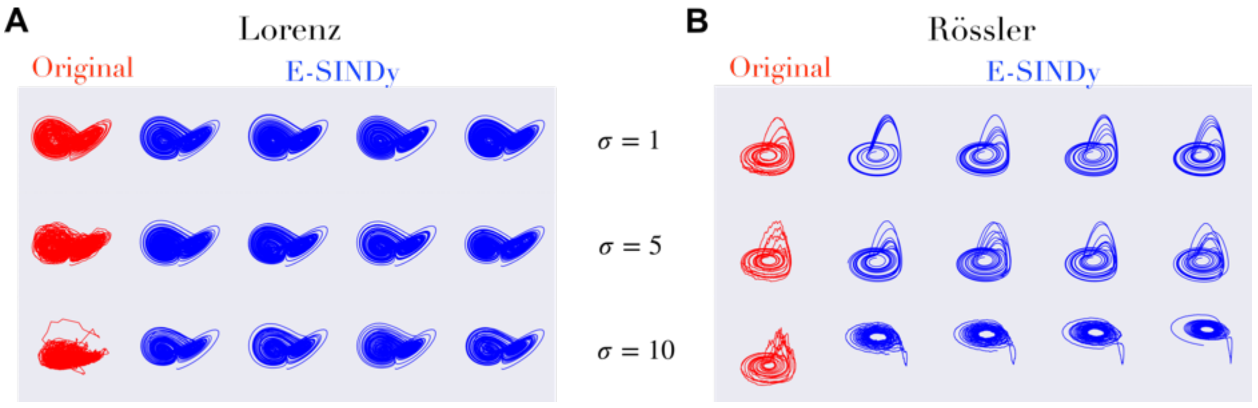

Figure 8: **E-SINDY 3D Stochastic Lorenz and Rössler Samples**. Samples generated using discovered E-SINDy equations for varying noise levels (σ).